Thin Solid Films, *70* (1980) 91–100

ELECTRICAL PROPERTIES OF VACUUM-DEPOSITED INDIUM OXIDE AND INDIUM TIN OXIDE FILMS

MAMORU MIZUHASHI
Research Laboratory, Asahi Glass Co., 1150 Hazawa, Kanagawa, Yokohama (Japan)
(Received November 14, 1979; accepted January 29, 1980)

Indium oxide films were deposited onto soda–lime glass substrates. The lowest resistivity found for indium tin oxide (ITO) films was 2×10^{-4} Ω cm with a carrier density n_e of 1×10^{21} cm^{-3} and a mobility μ_H of 30 cm^2 V^{-1} s^{-1} at the optimized doping level (5 wt.%) and substrate temperature (400 °C), whereas it was 4×10^{-4} Ω cm with $n_e = 4 \times 10^{20}$ cm^{-3} and $\mu_H = 72$ cm^2 V^{-1} s^{-1} for pure indium oxide films. The characteristic features of ITO films are their high carrier density and low mobility in comparison with ordinary electron-beam-deposited ITO films. It was determined from thermal stability tests that the contribution to the carrier density made by the addition of tin was at most $(3–4) \times 10^{20}$ cm^{-3}; *i.e.* the efficiency of generation of free carriers by the addition of tin is only a few tens of per cent.

1. INTRODUCTION

Extensive studies on indium tin oxide (ITO) thin film as a transparent conductor have been reported since the work of van Boort and Groth[1] on spray pyrolytic In_2O_3:Sn films, although the work of Rupprecht[2] (1954) is often still referred to. The work of van Boort and Groth has indicated for the first time that indium oxide appropriately doped with tin can have a resistivity ρ as low as 10^{-4} Ω cm, this value being fairly small compared with that of non-electrostatic shield formulation "A" (NESA) coating, SnO_2:Sb. At that time this low resistivity met the requirement for the electrodes of liquid crystal cells driven in the dynamic scattering mode.

Prior to the work of van Boort and Groth, Weiher had already reported[3] the electrical properties of single-crystal In_2O_3 grown on the inside wall of a crucible into which equal amounts of indium metal and carbon had been charged and heat treated at 1000 °C for 24 h and which had a loose cap to permit the gradual admission of oxygen. He found that the intrinsic donor levels lay 93 meV below the conduction band and the degeneracy began at a carrier density n_e of 1.48×10^{18} cm^{-3}.

Most of the ITO investigations carried out since then, however, have been based on films prepared by sputtering, so that relatively few data are available for the other methods, particularly for vacuum deposition, as has been pointed out in a recent review article[4]. Furthermore, there is a wide diversity in the optimized dopant concentration. This can be ascribed to differences in the deposition kinetics rather

than to the content of dopant in the film[4]. Although it is very difficult to separate the effects of deposition conditions on the electrical conduction process in ITO films, several discussions have been made on the basis of the controlled vacancy representation of Vincent[5]. According to Fan and Goodenough[6], conducting indium oxide can be expressed in the form In_2O_{3-2x}; thus it liberates $2x$ mol electrons. They have also suggested that shallow donor levels (0.03 eV) are formed by the In 5s electron orbital around the oxygen vacancies. With increase in number these donor levels form an impurity band and then overlap the conduction band at the onset of degeneracy. The addition of tin serves to form another impurity band below the conduction band by means of the Sn 5s orbitals. In other words, an Sn^{3+} ion on a lattice point is thermally excited to an Sn^{4+} ion and liberates a conduction electron. ITO thus can be represented in the form $In_{2-a}Sn_aO_{3-2x}$. There are $a+2x$ mol electrons in the crystal. Bosnell and Waghorne[7] consider that incorporated tin would exist as a lower oxide such as Sn_3O_4 so that it generates an oxygen vacancy. Agnihotri *et al.*[8] proposed the formula $(In_{1-x}Sn_x)_2O_{3-y}$, taking into account the substitution of In^{3+} with Sn^{2+}. The observed increase in resistivity for doping above the optimized level is explained in this model by the compensation of part of the donor levels of non-stoichiometric origin by an increment in Sn^{2+}, which makes the impurity band narrower and increases the activation energy for conduction.

From this discussion it is clear that the conduction mechanism is not yet fully understood. In particular the contributions of tin atoms and lattice defects such as donor impurities are, to the best of the author's knowledge, insufficiently recognized. The purpose of this paper is to report the general features of vacuum-evaporated indium oxide films together with an attempt to separate the contribution to the conductivity of In_2O_3:Sn films made by the addition of tin.

2. EXPERIMENTAL

In_2O_3 and SnO_2 were evaporated from two beryllia crucibles in the presence of oxygen. The partial pressure of the oxygen was of the order of 10^{-4} Torr. The crucibles were independently controlled to avoid fractionation and other possible effects when depositing from a single source containing premixed oxides. In order to increase the degassing capability in high vacuum ranges (10^{-5}–10^{-4} Torr) a NEVA model VI-502 evaporator equipped with an ion pump and a sublimation pump was connected to another diffusion-pump-based degassing line. A tantalum foil heater was used to avoid contamination of the indium oxide films because tantalum oxide has a fairly low vapor pressure compared with tungsten oxide or molybdenum oxide. The substrate was soda–lime glass unless otherwise specified.

The deposition rate was monitored with a quartz crystal monitor positioned beside the substrate. The distances to the substrate and between the two crucibles were 30 cm and 5 cm respectively. Deposition was carried out in the following manner. The two crucibles were heated to temperatures just below the onset of evaporation to soak and were maintained there for sufficient time nearly to attain thermal equilibrium with each other and the other equipment installed. After admitting oxygen to a predetermined pressure the deposition rate of In_2O_3 was increased to count the deposition rate r_{In} by raising the crucible temperature. The

SnO_2 crucible was then heated to count the total deposition rate $r_{total} = r_{In} + r_{Sn}$. This gives r_{Sn}/r_{In} which is a rough measure of the doping level.

The thickness was checked by Talystep 1. The composition of the films was determined from the fluorescent X-ray counting of tin or indium through Fig. 1, which was calibrated from the measured weight of SnO_2 or In_2O_3 films deposited on 0.8 mm thick microglass sheets. In the calibration work the weight of very thin SnO_2 films was determined by chemical analysis. The spectral transmission and reflection were measured with a Hitachi model EPS-III spectrometer. The electrical resistivity was doubly checked by the four-point probe method and the van der Pauw method. The Hall effect measurement was carried out in the van der Pauw configuration.

3. RESULTS AND DISCUSSION

3.1. Pure indium oxide films

The deposition of In_2O_3 films is reactive in nature because In_2O_3 decomposes to a suboxide when heated in a vacuum. Films are therefore non-absorbing only for a certain limited range of such deposition conditions as substrate temperature T_s, deposition rate r and oxygen partial pressure p_{O_2}. The absorption is a measure of the lower oxidation state of indium oxide. Figure 2 shows the relationship of the visible absorption A_v to the substrate temperature for films about 350 Å thick deposited under the conditions $r_{total} = 0.3$ Å s^{-1} and $p_{O_2} = 5 \times 10^{-5}$ Torr. Here A_v is defined as a fraction of the summation $\Sigma S_\lambda A_\lambda$ of the products of the sensitivity S_λ of the eye and the spectral absorption $A_\lambda = 1 - T_\lambda - R_\lambda$ divided by the summation ΣS_λ of the sensitivity of the eye. The visible absorption decreases with increasing T_s. There is no appreciable absorption for substrate temperatures higher than 400 °C.

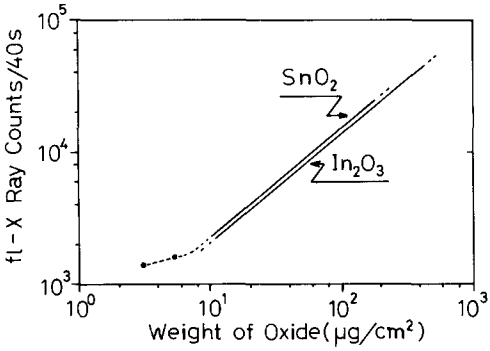

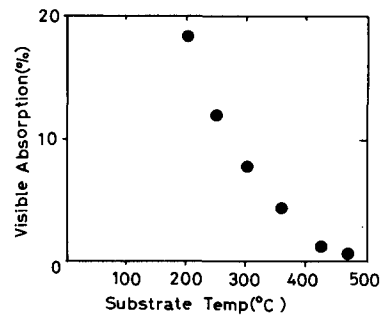

Fig. 1. Calibration to give the weight of the oxide film from the fluorescent X-ray counts of tin or indium at 40 kV and 40 mA with a chromium target 25 mm in diameter and a value for 2θ of 57.98° for tin and 55.06° for indium.

Fig. 2. Plot of the absorption A_v in the visible region as a function of the substrate temperature T_s for In_2O_3 films 350 Å thick deposited at $r_{total} = 0.3$ Å s^{-1} and $p_{O_2} = 5 \times 10^{-5}$ Torr.

Figure 3 shows the dependence on substrate temperature T_s of the electrical properties. The specific resistivity ρ decreases at first and then increases again as the substrate temperature is raised. As is indicated in the figure, the resistivity minimum at around 450 °C is caused by an increase in the mobility μ_H up to 450 °C and by a rapid decrease in the carrier density n_e at higher temperatures.

Figure 4 shows the spectral transmission and reflection of the pure indium oxide film with the lowest resistivity. This film was grown under the conditions $T_s = 420\,^{\circ}C$, $p_{O_2} = 1 \times 10^{-4}$ Torr and $r_t = 0.8$ Å s^{-1} to a thickness of 450 Å. Its electrical properties were $\rho = 4 \times 10^{-4}\ \Omega$ cm, $n_e = 3 \times 10^{20}$ cm^{-3} and $\mu_H = 72$ cm^2 V^{-1} s^{-1}. The as-deposited surface of this film had a hazy appearance caused by warped cylindrical deposits, as shown in Fig. 5(a); however, these could easily be wiped off as in Fig. 5(b). These deposits are assumed to be due to the decrease in the oxygen partial pressure at the later stage of deposition that arises because only the total pressure was kept constant despite the fact that there must be a steady increase in the partial pressure of non-oxidizing outgases from the inside wall during the deposition. In less oxidizing conditions the growth of a lower oxide film takes place. This probably gives rise to an additional stress in the film, resulting in stress-induced grain growth; we did not measure the stress in the film however.

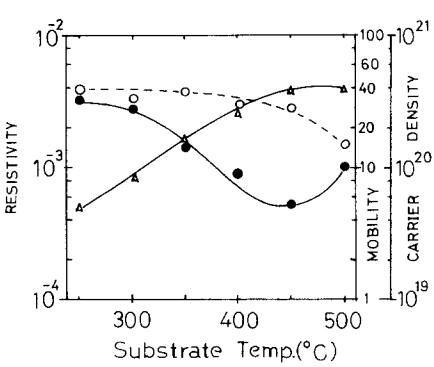

Fig. 3. Plots of the dependence of the electrical properties of In_2O_3 films on the substrate temperature T_s: ●, resistivity ρ; △, mobility μ_H; ○, carrier density n_e.

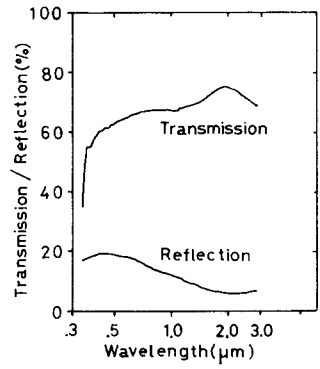

Fig. 4. Plots of the spectral transmission and reflection as a function of wavelength for the pure indium oxide film with the lowest resistivity, grown under the conditions $T_s = 420\,^{\circ}C$, $p_{O_2} = 1 \times 10^{-4}$ Torr and $r_t = 0.8$ Å s^{-1} to a thickness of 450 Å.

From Fig. 4 the optical constant $\tilde{n} = n - ik$ at $\lambda = 500$ nm was calculated to be given by $n = 1.96$ and $k = 0.13$. The refractive index is lower than those reported for sputtered ITO films[9]. The absorption coefficient, however, is very large[10], corresponding to $\alpha = 10^4$ cm^{-1}. It is difficult to give a satisfactory explanation of this high absorption and mobility because oxygen vacancies and interstitial indium atoms are responsible for both the light absorption and the generation and scattering of free carriers.

When the oxygen partial pressure p_{O_2} was raised to 2.5×10^{-4} Torr, roughly twice that in the previous case, with the other deposition conditions kept the same, the absorption vanished, as shown in Fig. 6, and the electrical properties on a fused quartz substrate were $\rho = 3 \times 10^{-2}\ \Omega$ cm, $n_e = 2 \times 10^{19}$ cm^{-3} and $\mu_H = 11$ cm^2 V^{-1} s^{-1}.

3.2. *In_2O_3:Sn films*

The specific resistivity of In_2O_3:Sn films obtained by the simultaneous evaporation of In_2O_3 and SnO_2 shows a minimum at a specific concentration of tin.

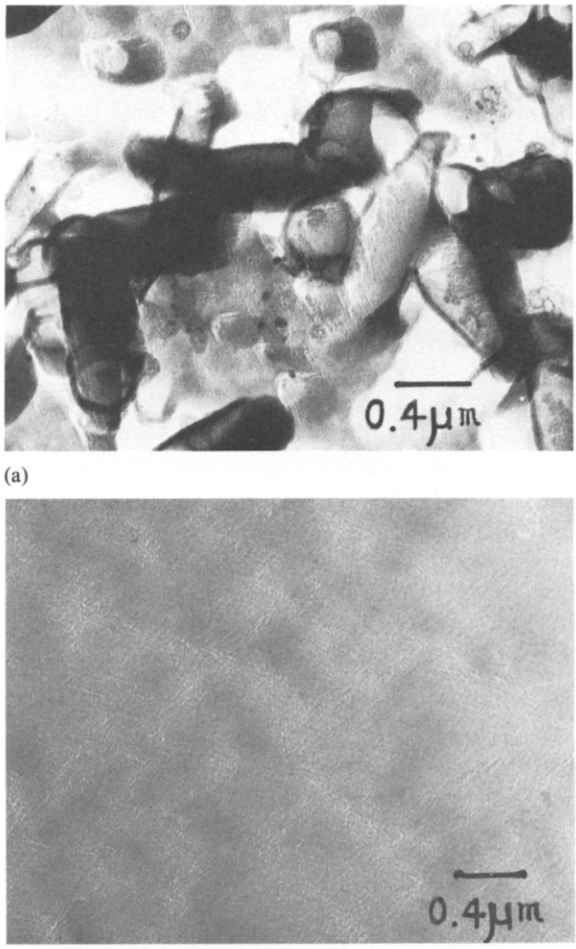

Fig. 5. Photomicrographs of the as-deposited surface of the pure indium oxide film of Fig. 4 (a) showing the warped cylindrical deposits and (b) after wiping.

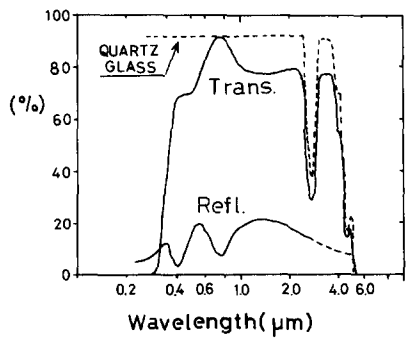

Fig. 6. Plots of the spectral transmission and reflection as a function of wavelength for a pure indium oxide film deposited under the conditions as in Fig. 4 but with $p_{O_2} = 2.5 \times 10^{-4}$ Torr.

Figure 7(a) shows the effect of the addition of tin for the case $T_s = 400\,^{\circ}C$, $p_{O_2} = 3 \times 10^{-4}$ Torr and $r_t = 0.8$ Å s^{-1}. An SnO_2 concentration of 4–6 wt.% gives a minimum resistivity because, as shown in the figure, the carrier density n_e has a maximum at this level of doping. This is in agreement with results for films deposited from a premixed oxide source[11]. A carrier density greater than 10^{21} cm^{-3} would reflect the contributions from oxygen vacancies and interstitial indium atoms as well as from substitutional Sn^{4+} ions. That the mobility decreases gradually at first, then rapidly, and that the carrier density decreases very fast for dopant concentrations of above 5 wt.% can be explained as follows. The addition of tin liberates a great many carriers at first but further addition inevitably causes disorders in the In_2O_3 lattice. Disorders enhance the scattering mechanisms such as phonon scattering and ionized impurity scattering, resulting in a decrease in mobility. A crystal lattice distorted too much in this way can no longer be effective either in generating Sn^{4+} ions on the substitutional sites of In^{3+} or in generating "effective" oxygen vacancies. The number of free carriers thus decreases sharply for dopant concentrations of more than 5 wt.%.

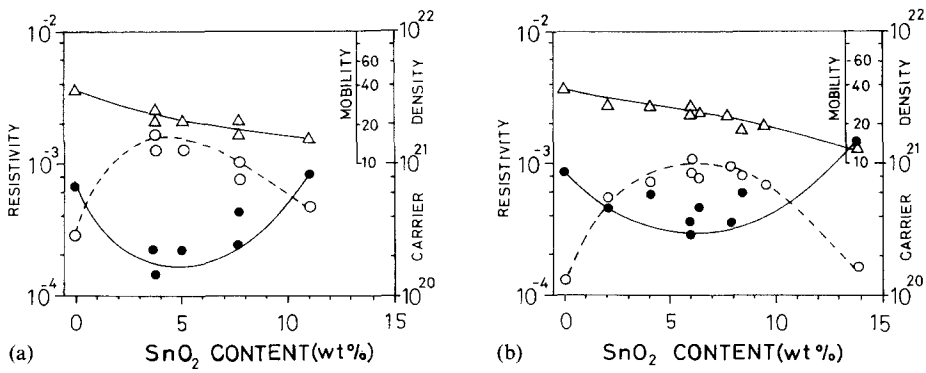

Fig. 7. Plots of the dependence of the electrical properties on the SnO_2 content for In_2O_3:Sn films deposited at $p_{O_2} = 3 \times 10^{-4}$ Torr, $r_t = 0.8$ Å s^{-1} and T_s = (a) 400 °C and (b) 450 °C: ●, resistivity ρ; △, mobility μ_H; ○, carrier density n_e.

Figure 7(b) shows the same relation for $T_s = 450\,^{\circ}C$. Higher substrate temperatures (higher by 50 °C) increased the mobility slightly but reduced the carrier density somewhat and furthermore shifted its peak position to a slightly higher tin concentration. This decrease in the carrier density raised the value of the resistivity minimum. The shift of the peak position toward higher doping levels and the broadening of its shape have been observed in SnO_2:Sb films[12], although no such shift was observed in spray pyrolytic ITO films[8]. Good crystallinity caused by a higher substrate temperature is responsible for these phenomena because of reduced phonon scattering. In addition there would be a good contact between crystallites owing to compressive stress[9] and to mechanisms which remove superfluous tin atoms from the crystal lattice when the film is formed on a high temperature substrate.

Figure 8 shows the substrate temperature dependence of the electrical properties of these films containing about 5 wt.% (4–6%) Sn. It is evident from the figure that the resistivity minimum lies in the range 400–450 °C where the

carrier density and the mobility show their maxima. It is noted that the film formed at $T_s = 200\,°C$ had rather a high carrier density and mobility, probably owing to a very low deposition rate which favors surface migration, oxidation and crystallization, although it was strongly absorbing ($A_v = 30\%$). It was also evident that a resistivity as low as $10^{-4}\,\Omega$ cm was easily attainable for $T_s > 400\,°C$ whereas it was difficult for $T_s < 350\,°C$. Surface haze was also observed in these In_2O_3:Sn films whenever the oxygen partial pressure was insufficient, for the same reason as in Section 3.1.

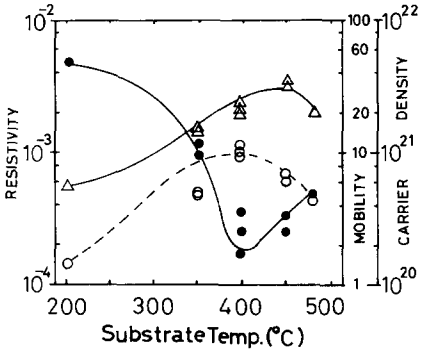

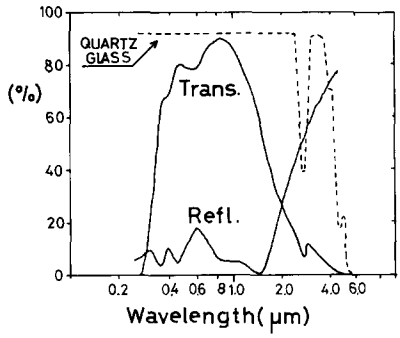

Fig. 8. Plots of the dependence of the electrical properties of In_2O_3:Sn films containing about 5 wt.% tin on the substrate temperature: ●, resistivity ρ; △, mobility μ_H; ○, carrier density n_e.

Fig. 9. Plots of the spectral transmission and reflection as a function of wavelength for an In_2O_3:Sn film 2500 Å thick doped with 6% Sn on a fused glass substrate.

Figure 9 shows the spectral transmission and reflection curves of a sample 2500 Å thick doped with 6% Sn on a fused quartz substrate. This film had electrical properties $\rho = 3.7 \times 10^{-4}\,\Omega$cm, $n_e = 3.8 \times 10^{20}\,cm^{-3}$ and $\mu_H = 43\,cm^2\,V^{-1}\,s^{-1}$ and was characterized by a wider band gap, no appreciable visible absorption and a sharp rise in reflectance at $\lambda \approx 1.5$ μm owing to free carrier absorption. Furthermore, the reflectance at the plasma absorption peak of nearly zero indicates a homogeneous growth of the film throughout the thickness. The optical energy gap, defined as the photon energy at which the absorption coefficient exceeds $1 \times 10^5\,cm^{-1}$, is from Fig. 9 about 4.1 eV, whereas that of less conductive film is from Fig. 6 3.85 eV. It is well known that the optical absorption edge E_{opt} of semiconductors is shifted to higher energies as the number of free carriers is increased. This is attributed to the Burstein effect[13] given by the expression

$$E_{opt} = E_g + \frac{h^2}{2m^*}\left(\frac{3n}{\pi}\right)^{2/3}$$

$$= E_g + \frac{h^2}{2}\left(\frac{1}{m_v} + \frac{1}{m_c}\right)\left(\frac{3n}{\pi}\right)^{2/3}$$

E_g is 3.75 eV [14]. The conduction electron mass m_c has been determined to be approximately $0.3m_0$ (ref. 15) and is negative, as noted by Ohhata and Yoshida[16]. The second term, the Burstein shift, is 1.4 eV for $n_e = 4 \times 10^{20}\,cm^{-3}$ and 0.19 eV for $n_e = 2 \times 10^{19}\,cm^{-3}$ when we put $m^* = 0.55m_0$ (ref. 3). Thus the calculated Burstein shift becomes too large at higher carrier densities. Detailed discussions would be

TABLE I

THE THERMAL DURABILITY OF THE ELECTRICAL PROPERTIES FOR VARIOUS HEAT TREATMENTS

Composition (wt.% SnO_2)	*Substrate temperature* (°C)	*Before treatment*			*After treatment*		
		ρ (Ω cm)	n_e (cm^{-3})	μ_H ($cm^2\ V^{-1}\ s^{-1}$)	ρ (Ω cm)	n_e (cm^{-3})	μ_H ($cm^2\ V^{-1}\ s^{-1}$)
					500 °C for 10 min		
Pure	500	9.4×10^{-4}	1.3×10^{20}	53.2	$1.8 \times 10^{+1}$	—	—
Pure	450	2.7×10^{-2}	2.1×10^{19}	10.9	$4.6 \times 10^{+2}$	—	—
5.7	400	4.6×10^{-4}	5.4×10^{20}	28.0	1.7×10^{-3}	3.6×10^{20}	10.5
8.6	450	2.7×10^{-4}	6.8×10^{20}	30.0	1.6×10^{-3}	3.3×10^{20}	12.1
12.6	400	1.9×10^{-3}	6.0×10^{20}	5.9	1.8×10^{-3}	4.3×10^{20}	8.2
					Room temperature, then 500 °C for 30 min		
20		2.2×10^{-3}	2.5×10^{20}	9.6	2.4×10^{-3}	2.3×10^{20}	9.5
					Room temperature, then 500 °C for 60 min		
					2.4×10^{-3}	2.3×10^{20}	9.6
					Room temperature, then 500 °C for 66 h		
					5.2×10^{-3}	2.4×10^{20}	5.1

necessary to establish the agreement between theory and experiment, although simple relations such as $E_{opt} \propto \sigma^{1/3}$ or $E_{opt} \propto n_e^{2/3}$ have been established[16,17].

Table I shows the changes resulting in the electrical properties of films heat treated at 500 °C for 10 min. This time interval is supposed to be long enough to complete the oxidation of films 600 Å thick. Pure In_2O_3 films show a drastic increase in resistivity by more than four orders of magnitude which is caused by the decrease in oxygen vacancies due to oxidation. In contrast, the mobility and the carrier density of doped films converge to $n_e = (3\text{–}4) \times 10^{20}$ cm^{-3} and $\mu_H = 10$ cm^2 V^{-1} s^{-1}. The samples in the last three rows of Table I give further information. They were deposited on a substrate at room temperature as a suboxide film then heat treated at 500 °C for 30 min before stability testing. The last two rows are the results of the prolonged stability testing of these post-oxidized ITO films. Heat treatment for more than 1 h decreased the mobility gradually, probably by causing the formation of scattering centers at grain boundaries[18]. As is shown in Table I, films oxidized from a suboxide have almost the same electrical properties as those oxidized from the state of high carrier density and high mobility.

From the foregoing discussion we can deduce that the carrier density $n_e = 3 \times 10^{20}$ cm^{-3} after testing at 500 °C probably corresponds to the effective contribution made by the addition of tin and thus the remaining contribution to the carrier density is from oxygen vacancies and other lattice defects. Only a few tens of per cent of the incorporated tin atoms are therefore effective in generating free carriers. There is no consensus about the distribution of the non-effective tin impurity in or among the indium oxide crystallites, although Sn^{2+} and Sn^{4+} states have been detected[6]. It would be very interesting to examine this problem.

We can also make another deduction from the comparison of the electrical properties on fused quartz, presented in Fig. 9, with those on soda–lime glass (Figs. 7(a) and 7(b)): there is almost no effect arising from the difference between the substrate glasses.

4. CONCLUSION

The lowest resistivities of vacuum-evaporated In_2O_3 and In_2O_3:Sn films were found to be 4×10^{-4} and 2×10^{-4} Ω cm with carrier densities of 3×10^{20} and 1×10^{21} cm^{-3} respectively. The optimized doping level of the tin impurity was about 5 wt.%, in good agreement with the results for ITO films deposited from a premixed oxide source. The contribution of impurity tin atoms to the conductivity was determined to be at the most 3×10^{20} cm^{-3}.

REFERENCES

1 H. J. J. van Boort and R. Groth, *Philips Tech. Rev.*, *29* (1968) 17.
2 G. Rupprecht, *Z. Phys.*, *139* (1954) 504.
3 R. L. Weiher, *Phys. Rev.*, *33* (1962) 2834.
4 J. L. Vossen, *Phys. Thin Films*, *9* (1977) 1.
5 C. A. Vincent, *J. Electrochem. Soc.*, *119* (1972) 515.
6 J. C. C. Fan and J. B. Goodenough, *J. Appl. Phys.*, *48* (1977) 3524.
7 J. R. Bosnell and R. Waghorne, *Thin Solid Films*, *15* (1973) 141.
8 O. P. Agnihotri, A. K. Sharma, B. K. Gupta and R. Tangaraj, *J. Phys. D*, *11* (1978) 643.

9 M. Just, N. Maintzer and I. Blech, *Thin Solid Films*, *48* (1978) 119.
10 W. W. Moltzen, *J. Vac. Sci. Technol.*, *12* (1975) 99.
11 H. Yoshida, H. Furubayashi, Y. Inoue and T. Tonomura, *Shinku*, *9* (1976) 13.
12 A. F. Carroll and L. H. Slack, *J. Electrochem. Soc.*, *123* (1976) 1889.
13 E. Burstein, *Phys. Rev.*, *93* (1954) 632.
14 R. L. Weiher and R. P. Ley, *J. Appl. Phys.*, *37* (1966) 299.
15 S. Noguchi, M. Mizuhashi and H. Sakata, *Rep. Res. Lab. Asahi Glass*, *28* (1978) 25.
16 Y. Ohhata and S. Yoshida, *Thin Solid Films*, *59* (1979) 255.
17 W. G. Haines and R. H. Bube, *Appl. Phys. Lett.*, *19* (1978) 304.
18 J. H. W. de Wit, G. van Unen and M. Lahey, *Phys. Chem. Solids*, *38* (1977) 819.